Electronic Supplementary Material (ESI) for Nanoscale.

Supporting Information

Electrochemically exfoliated from industrial ingot: ultrathin metallic bismuth nanosheets for excellent CO_2 capture and electrocatalytic conversion

Dan Wu, Xinquan Shen, Jianwen Liu, Cheng Wang, Yue Liang, Xian-Zhu Fu and Jing-Li Luo**

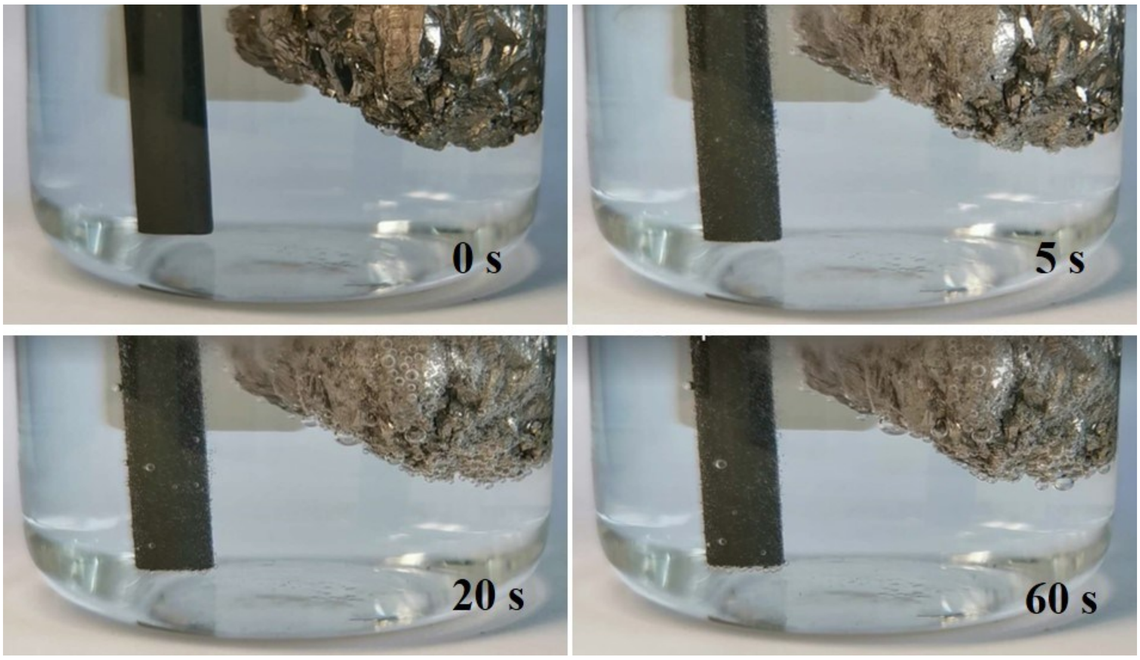

Figure S1. Digital photographs for the electrochemical exfoliation of Bi ingot at different times during synthesis in Na_2SO_4 aqueous solution (5 mg·mL^{-1}).

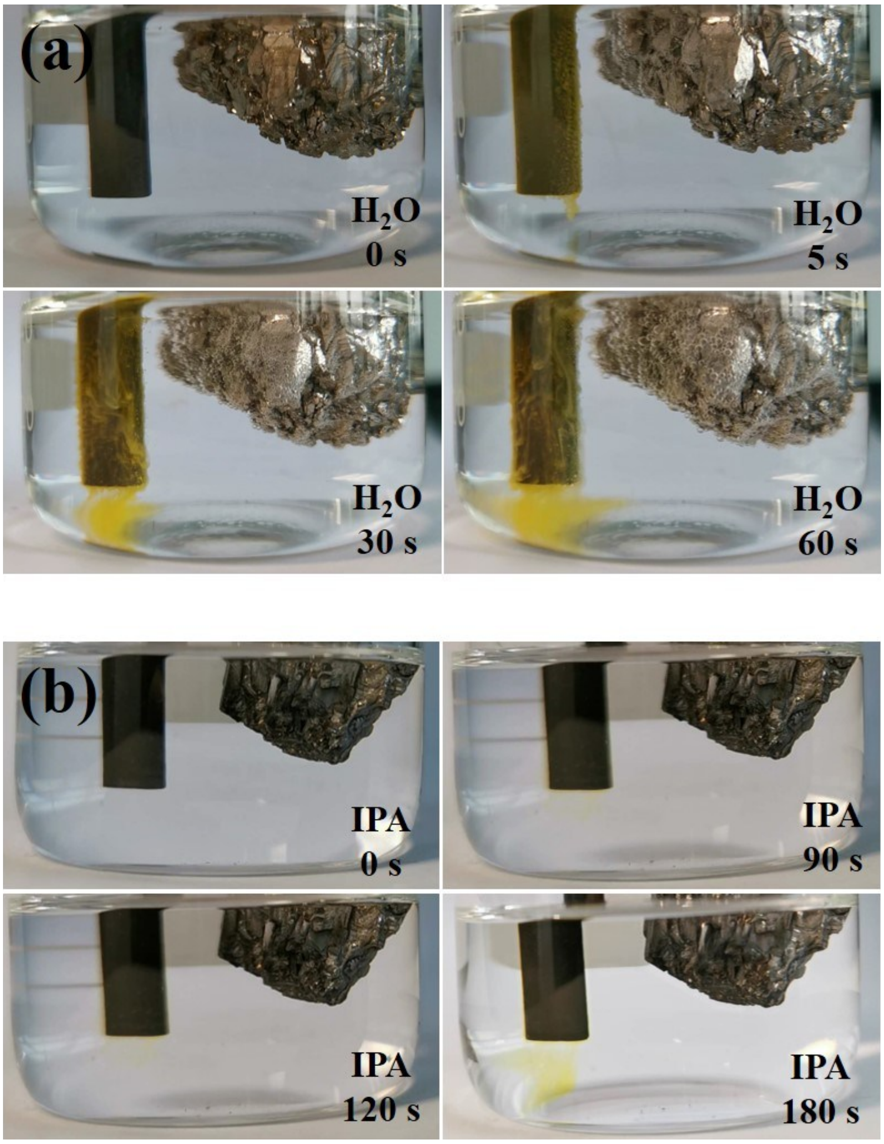

Figure S2. Digital photographs for the electrochemical exfoliation of Bi ingot at different times during synthesis with tetrapropylammonium bromide dissolved in (a) H_2O and (b) isopropyl alcohol (IPA) (5 mg·mL^{-1}) as the electrolyte.

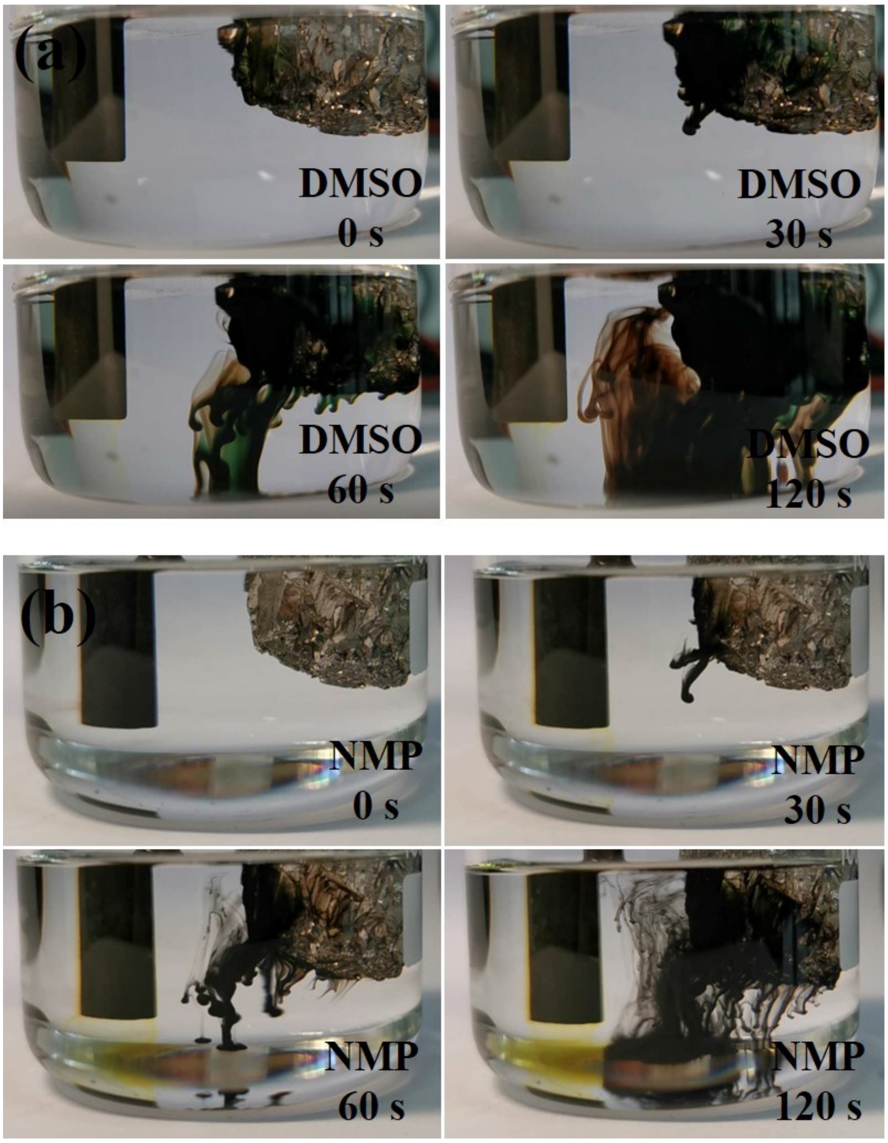

Figure S3. Digital photographs for the electrochemical exfoliation of Bi ingot at different times during synthesis with tetrapropylammonium bromide dissolved in (a) dimethyl sulfoxide (DMSO) and (b) 1-methyl-2-pyrrolidone (NMP) (5 mg·mL^{-1}) as the electrolyte.

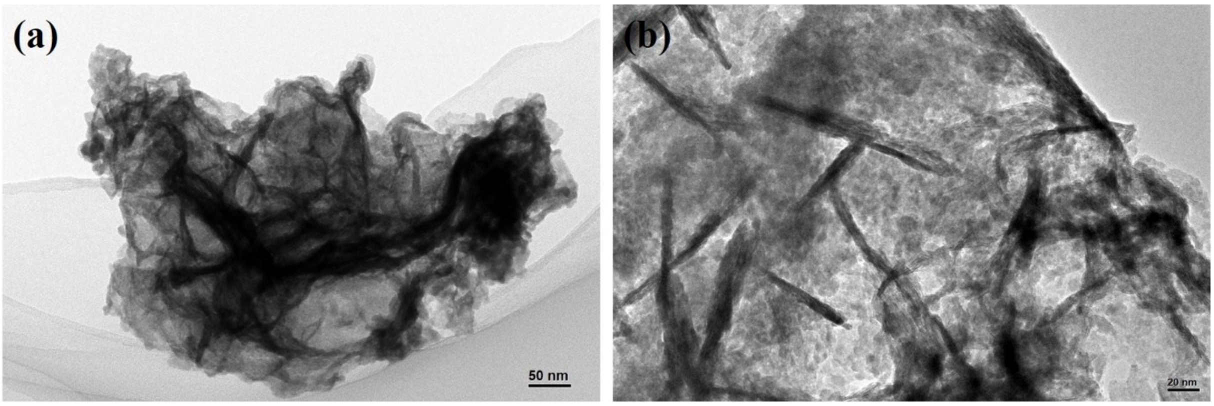

Figure S4. TEM images of Bi NS.

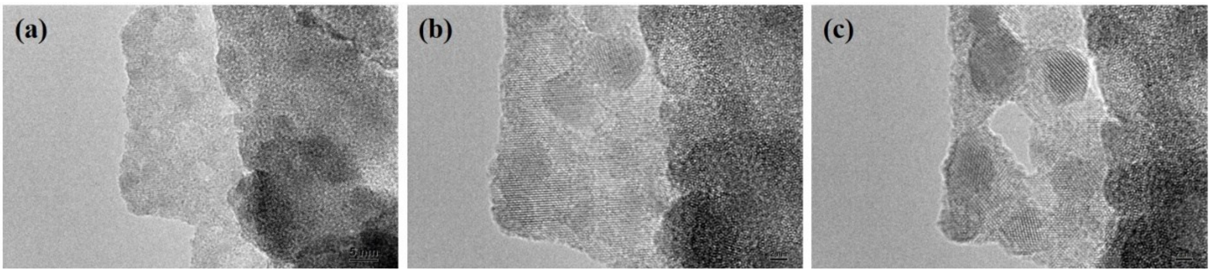

Figure S5. HRTEM images of Bi NS exposed under electron beam for (a) 30, (b) 40 and (c) 60 s.

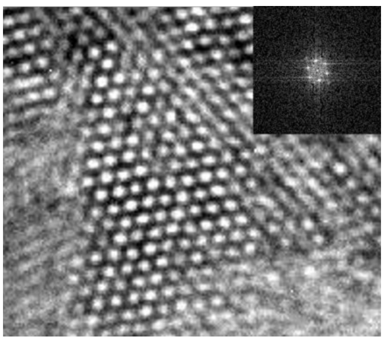

Figure S6. HRTEM image of Bi NS and corresponding FFT pattern.

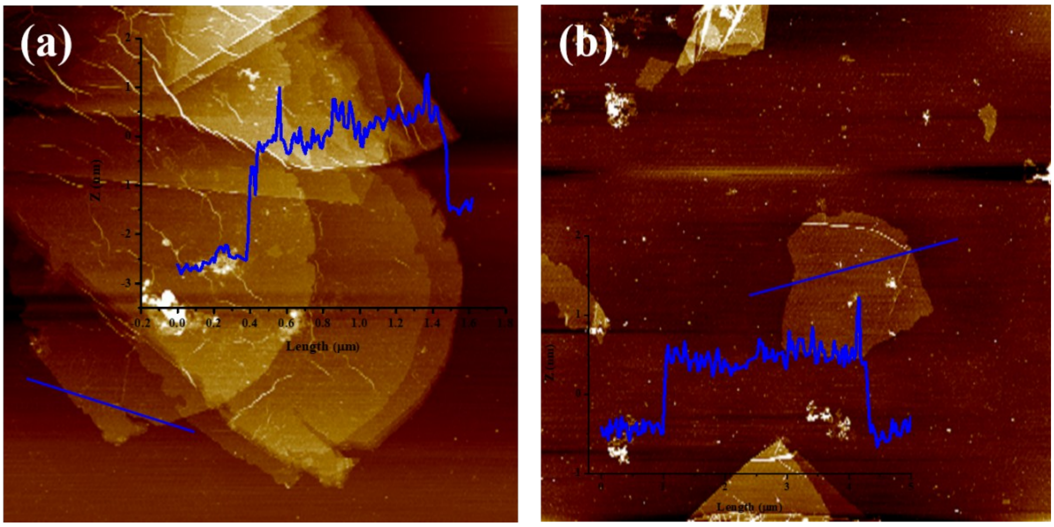

Figure S7. AFM images and corresponding height profile along the blue line of Bi NS.

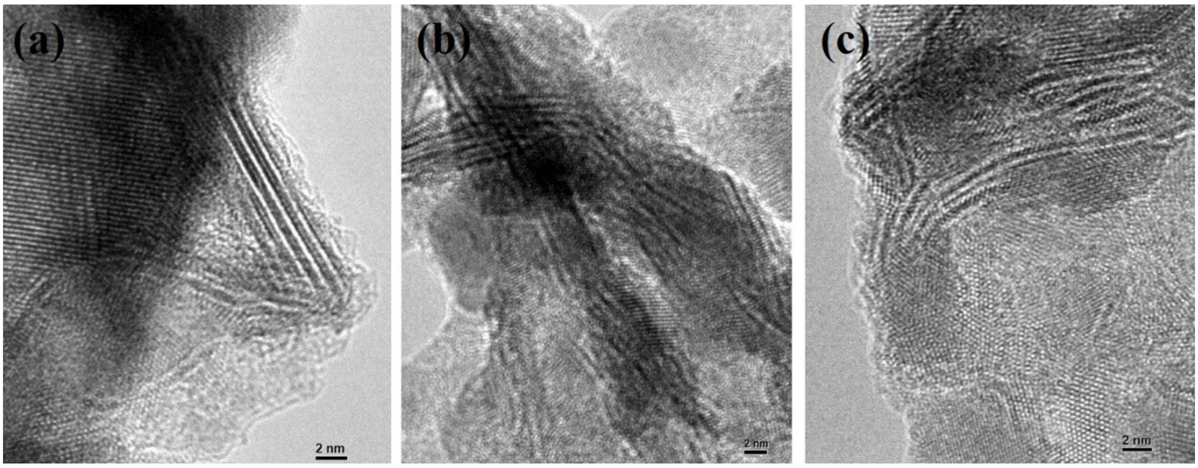

Figure S8. HRTEM images of Bi NS.

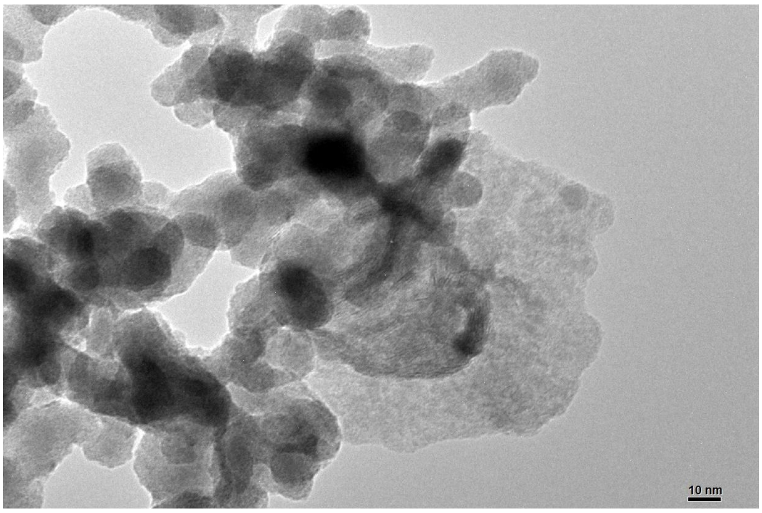

Figure S9. TEM image of Bi nanoparticles.

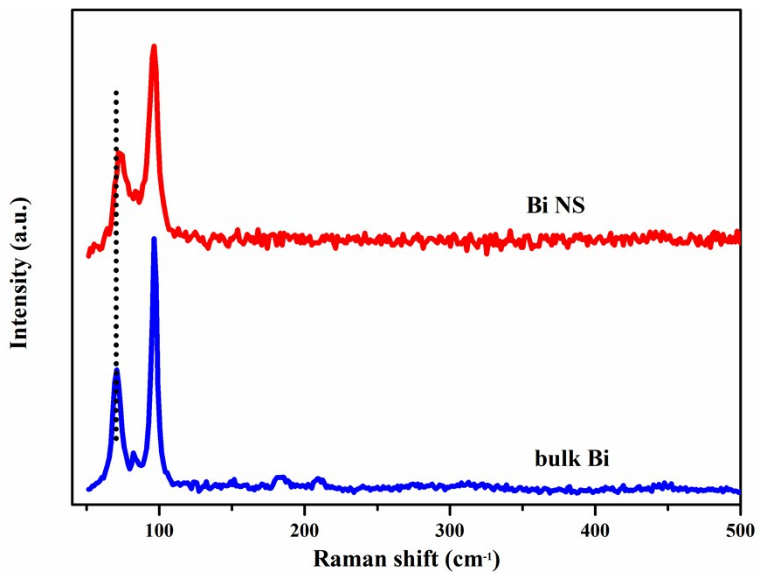

Figure S10. Raman spectra of Bi NS and bulk Bi.

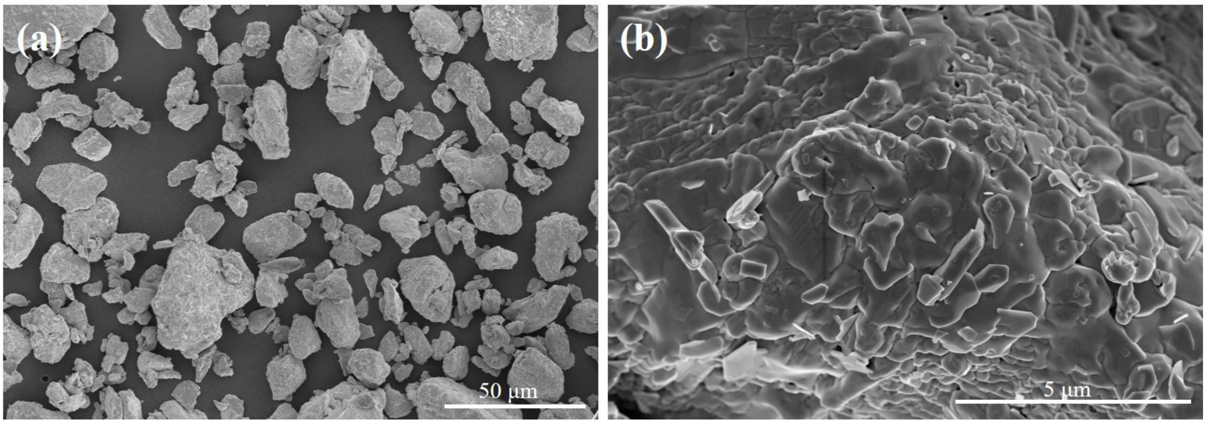

Figure 11. SEM images of commercial Bi powder (200 mesh).

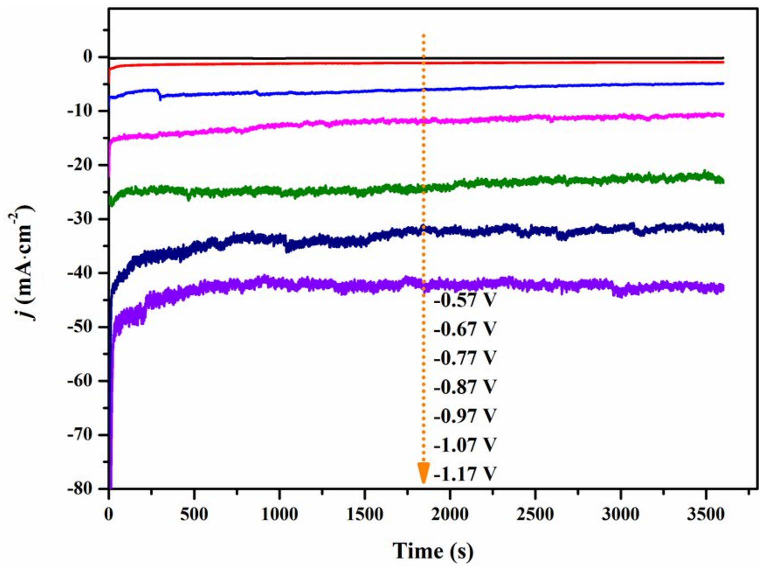

Figure S12. Constant-potential electrolysis on Bi NS in 0.5 M CO_2-saturated $KHCO_3$ for 1 h.

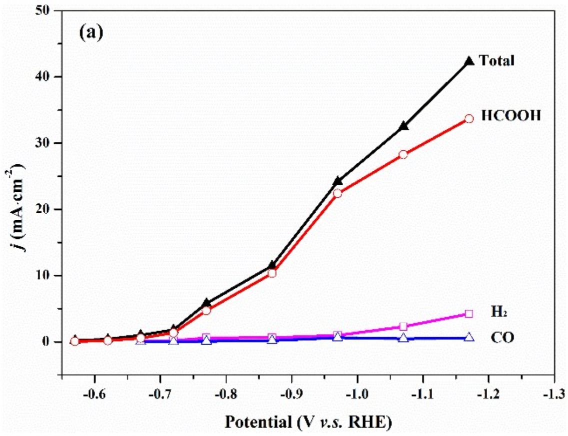

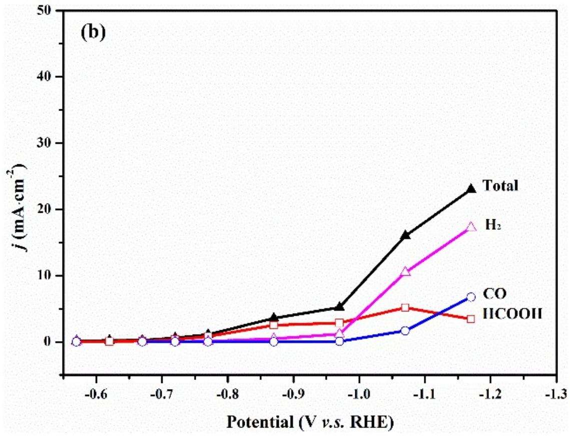

Figure S13. Total and partial current of HCOOH, H_2 and CO for (a) Bi NS and (b) Bi200 catalysts.

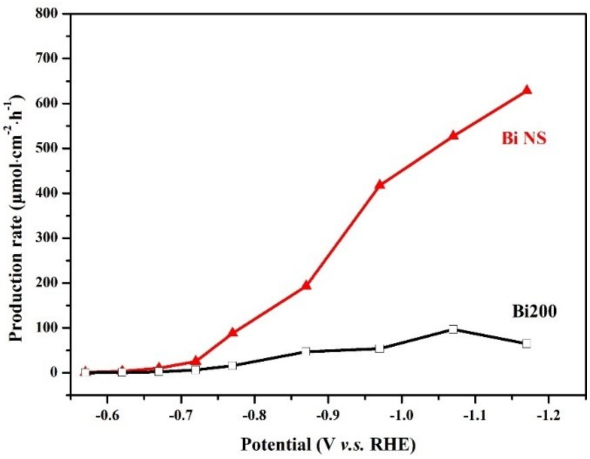

Figure S14. Production rate of HCOOH for Bi NS and Bi200.

Table S1 Comparison of catalytic performance in CO_2RR on Bi NS and recent reported Bi catalyst in the typical H-type system.

Catalyst	Supported substrate	Electrolyte	Maximum FE_{HCOOH}	j_{HCOOH} ($mA \cdot cm^{-2}$)	Reference
Bi nanosheets	with acetylene black on carbon paper	0.1 M $KHCO_3$	86% (-1.1 V)	14.2 (-1.1 V)	[1]
mesoporous Bi nanosheets	with Ketjenblack carbon on carbon paper	0.5 M $NaHCO_3$	99% (-0.9 V)	17 (-1.0 V)	[2]
Bi nanosheets	with Ketjenblack carbon on carbon paper	0.5 M $NaHCO_3$	100% (-0.93 V)	24 (-1.07)	[3]
nanotube Bi	with Ketjenblack carbon on carbon	0.5 M $KHCO_3$	93% (-0.7 V)	60 (-1.05 V)	[4]
Bi nanoflakes	Cu metal film	0.1 M $KHCO_3$	100% (-0.6 V)	14.9 (-1.2 V)	[5]
Bi dendrites	Cu foil	0.5 M $KHCO_3$	89% (-0.74 V)	2.7 (-0.74 V)	[6]
Bi nanowires	Cu foam	0.5 M $NaHCO_3$	95% (-0.69 V)	15 (-0.69 V)	[7]
Bi nanodendrites	carbon paper	0.5 M $KHCO_3$	96% (-1.13 V)	15.2 (-1.13 V)	[8]
Bi nanoparticles	carbon paper	0.5 M $KHCO_3$	95% (-0.83 V)	6.6 (-0.88 V)	[9]
Bi nanosheets	carbon paper	0.1 M $KHCO_3$	99% (-0.95 V)	50 (-0.9 V)	[10]
Bi nanosheets	carbon paper	0.5 M $NaHCO_3$	90% (-0.9 V)	3.9 (-0.8 V)	[11]
nano-Bi	glassy carbon electrode	0.5 M $KHCO_3$	98% (-0.93 V)	9.7 (-0.93 V)	[12]
rod-like Bi	glassy carbon electrode	0.5 M $KHCO_3$	84% (-0.75 V)	5 (-0.75 V)	[13]
POD-Bi	glassy carbon electrode	0.5 M $KHCO_3$	95% (-0.86 V)	18 (-0.86 V)	[14]
nano-Bi	gas diffusion electrode	0.5 M $NaHCO_3$	90% (-0.78 V)	1.5 (-0.78 V)	[15]
Bi NS	**carbon paper**	**0.5 M $KHCO_3$**	**93% (-0.97 V)**	**23 (-0.97 V)**	**This work**

FE_{HCOOH}: faradaic efficiency for HCOOH formation;

j_{HCOOH}: partial current density for HCOOH formation.

The potentials are converted to the RHE scale.

Table S2 Comparison of HCOOH production rate in CO_2RR for Bi NS and recent reported metal catalyst in the typical H-type system.

Catalyst	**Electrolyte**	**HCOOH production rate ($\mu mol \cdot cm^{-2} \cdot h^{-1}$)**	**Reference**
Bi nanoflakes	0.1 M $KHCO_3$	75 (-1.0 V)	[5]
Bi dendrites	0.5 M $KHCO_3$	50 (-0.74 V)	[6]
Bi nanoparticles	0.5 M $KHCO_3$	121 (-0.88 V)	[9]
nano-Bi	0.5 M $NaHCO_3$	30 (-0.78 V)	[15]
In	0.5 M $NaHCO_3$	136 (-1.5 V)	[16]
Sn	0.1 M $KHCO_3$	113.3 (-1.2 V)	[17]
Sn	0.1 M $NaHCO_3$	250 (-1.36 V)	[18]
Sn	0.1 M $KHCO_3$	229 (-1.36 V)	[19]
Bi NS	**0.5 M $KHCO_3$**	**460 (-0.97 V)** **700 (-1.17 V)**	**This work**

References in Supporting Information

[1] W.J. Zhang, Y. Hu, L.B. Ma, G.Y. Zhu, P.Y. Zhao, X.L. Xue, R.P. Chen, S.Y. Yang, J. Ma, J. Liu, Z. Jin. Liquid-phase exfoliated ultrathin Bi nanosheets: Uncovering the origins of enhanced electrocatalytic CO_2 reduction on two-dimensional metal nanostructure. Nano Energy 53 (2018) 808-816.

[2] H. Yang, N. Han, J. Deng, J.H. Wu, Y. Wang, Y.P. Hu, P. Ding, Y.F. Li, Y.G. Li, J. Lu. Selective CO_2 Reduction on 2D Mesoporous Bi Nanosheets. Adv. Energy Mater. 8 (2018) 1801536.

[3] N. Han, Y. Wang, H. Yang, J. Deng, J.H. Wu, Y.F. Li, Y.G. Li. Ultrathin bismuth nanosheets from in situ topotactic transformation for selective electrocatalytic CO_2 reduction to formate. Nat. Commun. 9 (2018) 1320.

[4] Q. Gong, P. Ding, M. Xu, X. Zhu, M. Wang, J. Deng, Q. Ma, N. Han, Y. Zhu, J. Lu, Z. Feng, Y. Li, W. Zhou, Y. Li. Structural defects on converted bismuth oxide nanotubes enable highly active electrocatalysis of carbon dioxide reduction. Nat. Commun. 10 (2019) 2807.

[5] S. Kim, W.J. Dong, S. Gim, W. Sohn, J.Y. Park, C.J. Yoo, H.W. Jang, J.L. Lee. Shape-controlled bismuth nanoflakes as highly selective catalysts for electrochemical carbon dioxide reduction to formate. Nano Energy 39 (2017) 44-52.

[6] J.H. Koh, D.H. Won, T. Eom, N.K. Kim, K.D. Jung, H. Kim, Y.J. Hwang, B.K. Min. Facile CO_2 Electro-Reduction to Formate via Oxygen Bidentate Intermediate Stabilized by High-Index Planes of Bi Dendrite Catalyst. ACS Catal. 7 (2017) 5071-5077.

[7] X.L. Zhang, X.H. Sun, S.X. Guo, A.M. Bond, J. Zhang. Formation of lattice-dislocated bismuth nanowires on copper foam for enhanced electrocatalytic CO_2 reduction at low overpotential. Energy Environ. Sci. 12 (2019) 1334-1340.

[8] H.X. Zhong, Y.L. Qiu, T.T. Zhang, X.F. Li, H.M. Zhang, X.B. Chen. Bismuth nanodendrites as a high performance electrocatalyst for selective conversion of CO_2 to formate. J. Mater. Chem. A 4 (2016) 13746-13753.

[9] X. Zhang, X.F. Hou, Q. Zhang, Y.X. Cai, Y.Y. Liu, J.L. Qiao. Polyethylene glycol induced reconstructing Bi nanoparticle size for stabilized CO_2 electroreduction to formate. J. Catal. 365 (2018) 63-70.

[10] F.P.G. de Arquer, O.S. Bushuyev, P. De Luna, C.T. Dinh, A. Seifitokaldani, M.I. Saidaminov, C.S. Tan, L.N. Quan, A. Proppe, M.G. Kibria, S.O. Kelley, D. Sinton, E.H. Sargent. 2D Metal Oxyhalide-Derived Catalysts for Efficient CO_2 Electroreduction. Adv. Mater. 30 (2018).

[11] P.P. Su, W.B. Xu, Y.L. Qiu, T.T. Zhang, X.F. Li, H.M. Zhang. Ultrathin Bismuth Nanosheets as a Highly Efficient CO2 Reduction Electrocatalyst. ChemSusChem 11 (2018) 848-853.

[12] Y. Qiu, J. Du, W. Dong, C. Dai, C. Tao. Selective conversion of CO_2 to formate on a size tunable nano-Bi electrocatalyst. J. CO_2 Utiliz. 20 (2017) 328-335.

[13] Y. Zhang, F.W. Li, X.L. Zhang, T. Williams, C.D. Easton, A.M. Bond, J. Zhang. Electrochemical reduction of CO_2 on defect-rich Bi derived from Bi_2S_3 with enhanced formate selectivity. J. Mater. Chem. A 6 (2018) 4714-4720.

[14] S.S. He, F.L. Ni, Y.J. Ji, L.E. Wang, Y.Z. Wen, H.P. Bai, G.J. Liu, Y. Zhang, Y.Y. Li, B. Zhang, H.S. Peng. The p-Orbital Delocalization of Main-Group Metals to Boost CO_2 Electroreduction. Angew. Chem. Int. Edit. 57 (2018) 16114-16119.

[15] X. Zhang, T. Lei, Y. Liu, J. Qiao. Enhancing CO_2 electrolysis to formate on facilely synthesized Bi catalysts at low overpotential. Appl. Catal. B: Environ. 218 (2017) 46-50.

[16] R. Hegner, L.F.M. Rosa, F. Harnisch. Electrochemical CO_2 reduction to formate at indium electrodes with high efficiency and selectivity in pH neutral electrolytes. Appl. Catal. B: Environ. 238 (2018) 546-556.

[17] B. Qin, H. Wang, F. Peng, H. Yu, Y. Cao. Effect of the surface roughness of copper substrate on three-dimensional tin electrode for electrochemical reduction of CO_2 into HCOOH. J. CO_2 Utiliz. 21 (2017) 219-223.

[18] V.S.K. Yadav, Y. Noh, H. Han, W.B. Kim. Synthesis of Sn catalysts by solar electro-deposition method for electrochemical CO_2 reduction reaction to HCOOH. Catal. Today 303 (2018) 276-281.

[19] H. Won da, C.H. Choi, J. Chung, M.W. Chung, E.H. Kim, S.I. Woo. Rational Design of a Hierarchical Tin Dendrite Electrode for Efficient Electrochemical Reduction of CO_2. ChemSusChem 8 (2015) 3092-3098.